sustainability

MDPI

Article

Robust Design of Power System Stabilizers Using Improved Harris Hawk Optimizer for Interconnected Power System

Lakhdar Chaib [1], Abdelghani Choucha [1], Salem Arif [1,2], Hatim G. Zaini [3], Attia El-Fergany [4] and Sherif S. M. Ghoneim [5,*]

1 Energy and Materials Laboratory, University of Tamanghasset, P.O. Box 10034 Sersouf, Tamanghasset 11001, Algeria; l.chaib@lagh-univ.dz (L.C.); a.choucha@lagh-univ.dz (A.C.); s.arif@lagh-univ.dz (S.A.)
2 LACoSERE Laboratory, Electrical Engineering Department, Amar Telidji University of Laghouat, P.O. Box 37G, Laghouat 03000, Algeria
3 Computer Engineering Department, College of Computer and Information Technology, Taif University, Al Huwaya, Taif 26571, Saudi Arabia; h.zaini@tu.edu.sa
4 Electrical Power and Machines Department, Faculty of Engineering, Zagazig University, Zagazig 44519, Egypt; el_fergany@ieee.org
5 Department of Electrical Engineering, College of Engineering, Taif University, Taif 21944, Saudi Arabia
* Correspondence: s.ghoneim@tu.edu.sa

Abstract: In this present work, a new metaheuristic method called a Harris hawk optimizer (HHO) is applied to achieve the optimal design of a power system stabilizer (PSS) in a multimachine power system. Several well-known chaos maps are incorporated into the HHO to form a chaotic HHO (CHHO) with the aim of improving static operators and enhancing global searching. To assess the CHHO performance, exhaustive comparison studies are made between anticipated chaotic maps in handling unconstrained mathematical problems. At this moment, The PSS design problem over a wide permutation of loading conditions is formulated as a non-linear optimization problem. The adopted objective function defines the damping ratio of lightly damped electromechanical modes subject to a set of constraints. The best PSS parameters are generated by the proposed CHHO. The applicability of the proposed CHHO based on PSS is examined and demonstrated on a 10-generator and 39-bus multimachine power system model. The performance assessments of the CHHO results are realized by a comparative study with HHO through extensive simulations along with further eigenvalue analysis to prove its efficacy. The simulation results convincingly demonstrate the high performance of the proposed CHHO-PSS under various operating scenarios.

Keywords: power system stability; multimachine power system model; power system stabilizer; chaotic Harris hawk optimization algorithm

check for updates

Citation: Chaib, L.; Choucha, A.; Arif, S.; Zaini, H.G.; El-Fergany, A.; Ghoneim, S.S.M. Robust Design of Power System Stabilizers Using Improved Harris Hawk Optimizer for Interconnected Power System. *Sustainability* **2021**, *13*, 11776. https://doi.org/10.3390/su132111776

Academic Editor: Mohammed Lotfy

Received: 23 September 2021
Accepted: 22 October 2021
Published: 25 October 2021

Publisher's Note: MDPI stays neutral with regard to jurisdictional claims in published maps and institutional affiliations.

Copyright: © 2021 by the authors. Licensee MDPI, Basel, Switzerland. This article is an open access article distributed under the terms and conditions of the Creative Commons Attribution (CC BY) license (https://creativecommons.org/licenses/by/4.0/).

1. Introduction

Due to the fast growth of power demand in recent years, the inadequacy of resources increases the complexity and remoteness of power systems. Accordingly, heavy loads are being imposed on the existing power system [1]. The stability of power systems defines the tendency and capacity of the power system to expand its restoration by keeping its equilibrium state after disturbances without extended loss of synchronism [2]. Damping of power system oscillations in a multimachine power system is extremely essential for the system operation security. As a result, a power system stabilizer (PSS) has been typically used to damp out the generator's electromechanical oscillations modes in electric power systems [1–3].

In the last decade, artificial intelligence has been introduced to design PSSs such as artificial neural networks [4–7], fuzzy logic [8,9], adaptive fuzzy in [10,11], and neuro-fuzzy in [12]. These proposed methods have demonstrated the performance to damp out the power system oscillations compared with the power system stabilizer. In addition, these

approaches permit the implementation of a PSS including the parameter uncertainty and non-linearity of the power system and further supply the best signal efficiency for a large limit of loading conditions. A fuzzy logic PSS based on learning and evolution is proposed in [13], which is a hybrid technique that the coordinate evolution and learning that is implemented whereby each one complements the other's potency.

The optimal parameters tuning of PSS in power system stability have been reported in the literature based on many optimization algorithms (conventional and recent based algorithms). It can be concluded that conventional optimization techniques such as the simplex and the gradient descent methods are not able to supply an appropriate solution. The key reason is that these algorithms need additional information, and are simply being trapped in the local solutions to extremely complex problems.

In the last two decades, several modern algorithms have widely evolved that easily solve optimization problems that were hard to get solutions to before. Amid these algorithms are the genetic algorithm (GA), particle swarm optimization (PSO), evolutionary algorithm, differential evolution (DE), bat algorithm (BA), and many more. Several articles are dedicated to designing the PSS using the mentioned algorithms that should be used for developing the power system reliability. The effectiveness of the GA in improving power system stability has been reported in several studies [2,3,14–17]. The advantage of the GA in relation to other optimization techniques is to be independent of the complexity of problems. PSOs have been investigated in the literature for PSS robust setting in a multimachine power system [17–19], to improve power system stability and enhance the damping of electromechanical oscillations of power systems. To attain the same goal, the parallel vector evaluated improved honey bee mating optimization [16,20].

Many new optimization algorithms have been proposed for ensuring the best setting in the power system. These algorithms have the ability to augment the global search algorithm. The power system stability improvement using these algorithms is presented in many papers. Teaching-learning-based optimization is also employed [21], fertility algorithms [22] are addressed, as well as Whale optimization algorithm [23]. In Ref. [24], the design of a conventional PSS is performed by the bat algorithm to set its pole-zero and gain parameters. The suggested technique of PSS design is transformed with an objective fitness including an eigenvalue system to guarantee the damping of the test system for a wide limit of loading conditions of the model. On the other hand, the BA is suggested in [25] for the robust design of PSS in the power system of multi-machine. In addition, a novel structure of PSS has also been investigated [26] for the first time, using a BA to improve power system stability.

Cyber security is getting to be a major concern to power system frameworks as the operation of a power system is extremely attached to cyber communication. As a result, it is necessary to seek and study the effect of cyber-attacks on the modern power system. The progress of a reliable power system needs a deeper perception of potential effects resulting from successful cyber-attacks. Estimating practical attack effects stands in need of an assessment of the grid's reliance on its cyber foundation and its capacity to endure potential failure. The investigation of the cyber-physical interaction inside the power system is essential to establish the adequacy of cyber-security efforts at enhancing the power system stability [27,28].

In this work, an improvement to the Harris Hawks Optimizer (HHO) is incorporated to achieve a robust algorithm to confidently produce parameters of PSS. Later in the text of this article, this proposed novel algorithm is called CHHO. Several chaos maps are attempted and the optimal one is chosen. Various operating loading scenarios are proposed with detailed discussions and analyses. Comparisons among standard HHO besides other well-known comparative algorithms and the proposed CHHO are made to signify the value of the proposed CHHO-PSS control strategy.

HHO is easy to develop because of its simple structure with high flexibility and easiness of implementation. HHO has simple operations with few tuned parameters. Therefore, the modified HHO can successfully be employed in various power system

troubles, as well as to get the best controller gains. It is anticipated that efficient approaches such as chaotic maps acquire high superiority solutions for tackling the desired power output in different scenarios. In this article, the below noteworthy features can be stated in order to report on numerically throughout this paper:

An efficiency improvement of a powerful metaheuristic method named the HHO is investigated to achieve a set of optimal proposed controllers.

A chaotic HHO called (CHHO) is proposed by hybridizing several chaotic sequences in HHO to enhance the global convergence and find the optimal solution, as well as to run away from local convergence.

The combination of chaotic maps with HHO generates another search space distinguished to original HHO operations that ensure the best performance in improving power system stability thus best results are established.

The structure of this article is organized as follows; in addition to this introduction section, Section 2 presents the problem statement including the description of the power system model with the study system, and the PSS structure and objective function are also described. Section 3 announces a review of the proposed algorithms with our improvement to the standard HHO. In Section 4, the effectiveness of the proposed stabilizer is tested under different cases and compared with the PSS-based HHO. In addition, the comparison is extended between CHHO, HHO, and DE under eigenvalue analysis to prove the effectiveness of this proposition. At last, the concluding remarks are drawn in Section 5.

2. Problem Statement and Modeling

2.1. Power System Modeling

In this study, a fourth-order model to represent the synchronous machine is used. The power system can be formulated as depicted in (1).

$$\dot{X} = f(X, U) \tag{1}$$

where X defines the vector of the state variables and U denotes the vector of the input variable. The state vector of n generators is given as $\left[\omega_i \ \delta_i E'_{qi} \ E_{fdi}\right]^T$ and U is the PSS output signal. This model is widely used in the analysis of parameter values settings of PSS [29].

$$\begin{cases} \dot{\omega_i} = \frac{(P_m - P_e - D\omega)}{M} \\ \dot{\delta_i} = \omega_0(\omega - 1) \\ \dot{E'_{qi}} = \frac{\left(-E_q + E_{fd}\right)}{T'_{do}} \\ \dot{E_{fdi}} = \frac{-E_{fd} + K_a\left(V_{ref} - V_t\right)}{T_a} \end{cases} \tag{2}$$

In studies of dynamic stability, the linearization model of the power system is applied around its operating point. The state equations of the power system can be written as follows:

$$\dot{X} = AX + BU \tag{3}$$

where A is a $4n \times 4n$ matrix and is given by $\partial f / \partial X$, while B is the input matrix with order $4n \times m$ and is given by $\partial f / \partial U$. The A and B are calculated with each operating point. The state vector X has an order of $4n \times 1$ and the input vector U has an order of $m \times 1$.

Figure 1 depicts the generalized multimachine power system scheme.

2.2. System under Study

A multi-machine IEEE 39-bus system is investigated in this work to appraise the coherency of the suggested scheme which is well known as a 10-machine New-England power system. The aggregation of a large number of generators is generator 1. All generators are equipped with PSS. The system data can be found in Ref. [30] while Figure 2 reveals the single line diagram of the power system under study.

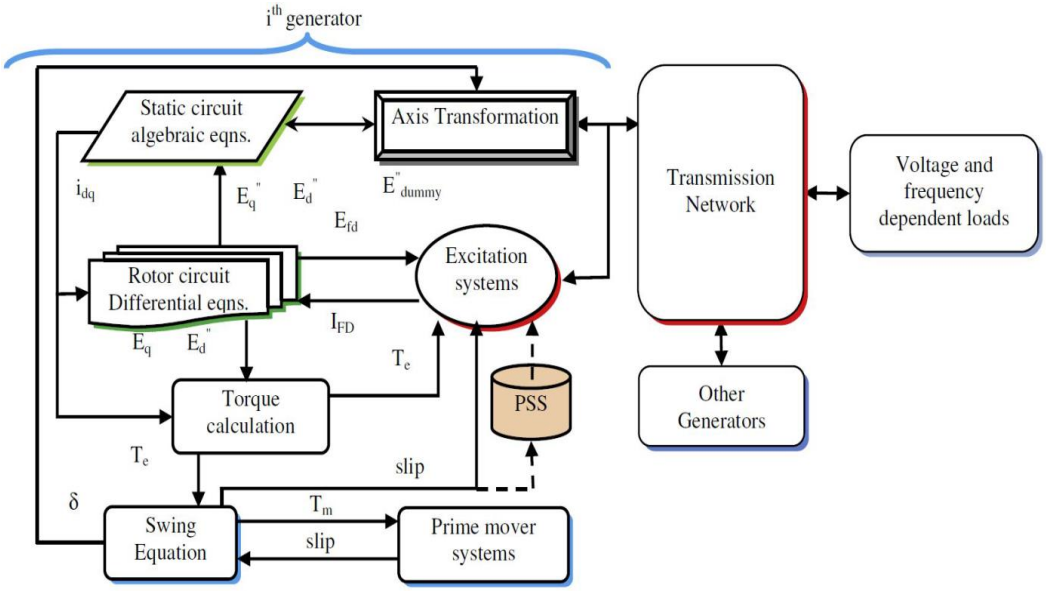

Figure 1. Multimachine power system scheme.

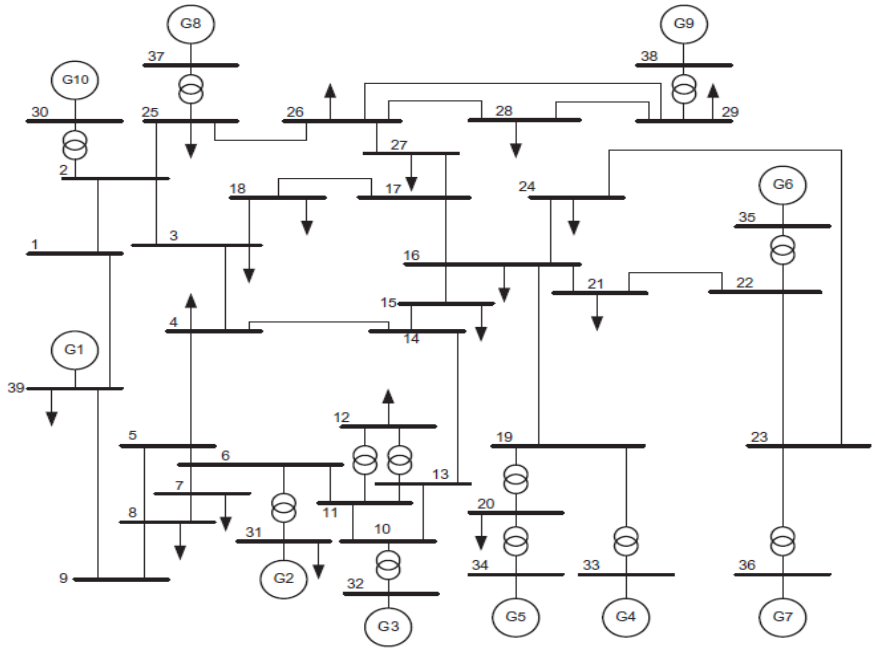

Figure 2. Single line diagram of Ten-generator thirty-nine-bus new-England power system.

2.3. Power System Stabilizer

The conventional structure of the PSS is used in this study as shown in Figure 3, and its transfer function is given by Equation (4) [31,32]. PSS comprises a block of K gain followed by a high-pass filter of time constant T_w and a lead-lag structured phase compensation blocks with time constants: T_1, T_2, T_3, and T_4. It is important to remind that the suggested stabilizers are designed to reduce the system oscillations under severe perturbations with a view to enhance the dynamic stability. The output stabilizer ΔV_{PSS} is a voltage signal that is added to the input voltage signal of the exciter system. The input signal of such a structure is usually the deviation of the synchronous speed $\Delta\omega$. It can be displayed the transfer function as hereunder:

$$\Delta V_{PSS} = K\frac{sT_W}{(1+sT_W)}\left[\frac{(1+sT_1)}{(1+sT_2)}\frac{(1+sT_3)}{(1+sT_4)}\right]\Delta\omega \quad (4)$$

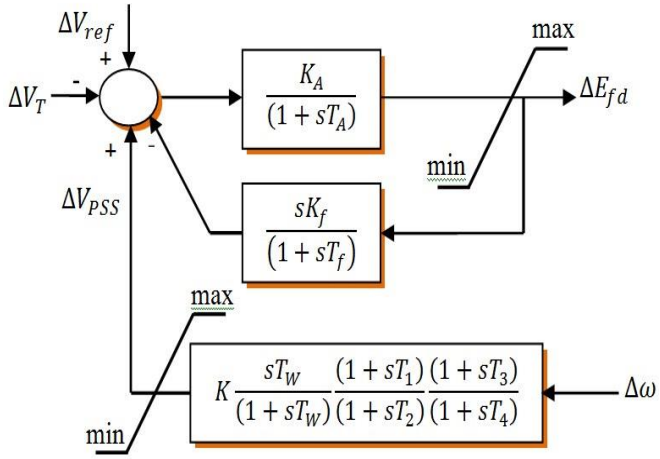

Figure 3. Conventional Power System Stabilizer (Lead-lag) with an excitation system.

2.4. Problem Formulation and the Objective Function

The foremost formative of PSS design inhabits the parameters altering its blocks, and even the damping of electromechanical modes will significantly augment. So far, the main aim of this section to determine the optimal parameter values of PSS that provide satisfactory damping oscillations rotor and ensure the overall stability of the system for different operating points as given in this work. The best PSS parameters allow modulating the excitation system via AVR to mitigate the small-signal oscillation. Progressively, the CHHO algorithm was applied to maximize the value of the damping ratio provided by the objective function (F) of the power system as much as possible. Throughout this study, the optimization problem is then formulated as follows:

$$F(K_m, T_{1m}, T_{2m}, T_{3m}, T_{4m}) = max(min(\xi_i)) \tag{5}$$

$$\begin{cases} \lambda_i = \sigma_i \pm j\omega_i \\ \xi_i = \frac{-\sigma_i}{\sqrt{{\sigma_i}^2+{\omega_i}^2}} \end{cases} \tag{6}$$

where λ_i and ξ_i are the eigenvalues and damping ratios of the i^{th} mode respectively, σ is the system real part of the poles, and ω is the pulse oscillation.

It should be mentioned that the parameters of PSS are typically restricted within which the PSS must encase the electromechanical oscillation frequency between 0.1–3 Hz [29]. Therefore, there are three parameters to be optimized here for each PSS (a gain and two time constants), and they are subject to the following constraints:

$$\begin{cases} 1 \le K_m \le 100 \\ 0.01 \le T_{1m} \le 2 \\ 0.01 \le T_{2m} \le 2 \\ 0.01 \le T_{3m} \le 2 \\ 0.01 \le T_{4m} \le 2 \end{cases} \tag{7}$$

where F is the objective function and m is the PSS index corresponding to the m generator of the system. In this study, the other parameters T_W is considered constant in a way that $T_W = 10$ to reduce the time computation and covers the mentioned oscillations, as well as to limit the search space to avoiding the worst fitness values by decreasing the optimized parameters.

3. Proposed Algorithm and Solving Methodology

3.1. Harris Hawks Optimizer

The authors have applied a nature-inspired optimization algorithm called HHO developed in Ref. [33] and inspired by the behavior of Harris hawk birds [33,34]. The

main process of the algorithm relies on the collaboration between hawks in the phase of hunting their prey. According to this algorithm, the Harris hawks group hit the prey from several directions to get it all of a sudden. Obviously, the escape manner of prey is comparable to the Harris hawk's chase pattern. Birds collaborate between them during the attack procedure. Concurrently, the target prey is attacked by the group leader of the Harris hawks, who pursues it and suddenly disappears from sight, and the next Harris hawk keeps up the chase.

The HHO algorithm is a global optimizer and better than other well-known algorithms based on its applicability to different real problems. Moreover, HHO can establish a balance between exploitation and exploration phases and maintain them in a stable manner. Profoundly, the HHO algorithm has a configuration comprising three phases. The first one is the exploration capability, which is expressed as follows:

$$x(t+1) = \begin{cases} x_{rand}(t) - r|x_{rand}(t) - 2r_2x(t)|q \geq 0.5 \\ x_{prey}(t) - x_a(t) - r_3(LB + r_4UB - LB))q < 0.5 \end{cases} \quad (8)$$

where $X(t)$ presents the hawk's current location, $X(t+1)$ also presents the hawk's location in the next generation t, $X_{prey}(t)$ denotes the prey location, r_1, r_2, r_3, r_4 and q are random parameters in the range of $(0, 1)$. $X_{rand}(t)$ is the randomly chosen hawk from the population. Additionally, LB and UB are, respectively, the lower and upper bounds. $X_a(t)$ means the average position of the Harris hawk, which is formulated as:

$$x_a(t) = \frac{1}{N}\sum_{i=1}^{N} x_i(t) \quad (9)$$

where $x_i(t)$ considers the location of each Harris hawk in generation t and N presents the number of all Harris hawks.

The exploitation is the second phase in HHO. Obviously, during the chase and hunt, the hawks' energy is decreased. The prey's energy can be exposed as follows:

$$E = 2E_0\left(1 - \frac{1}{T}\right) \quad (10)$$

T is the maximum number of generations, E_0 indicates the energy in the first stage while E designates the escaping energy. Throughout this phase, when $|E_0| \geq 1$ and $|E_0| < 1$, the exploration is happening and has occurred, respectively.

The exploitation indicates the final phase, which is employed to enhance the local solutions compared to previously achieved solutions. During this phase, the hawks' surprising attack on the prey was identified in the preceding two phases. Based on the prey's escape and hawks' chasing, the problem is formulated.

3.1.1. Soft Besiege

The validation of the soft besiege condition is occurs when $r \geq 1$ and $|E_0| \geq 0$, which is defined as:

$$x(t+1) = \Delta x(t) - E\left|Jx_{prey}(t) - 2x(t)\right| \quad (11)$$

$$\Delta x(t) = x_{prey}(t) - x(t) \quad (12)$$

where Δx denotes the difference between the current location and the prey location. J is the random jump power and equals to $J = 2(1 - r_5)$, and r_5 is a random value between 0 and 1.

3.1.2. Hard Besiege

The besiege condition is employed when $r \geq 0$ and $|E_0| < 0$. The prey in this phase does not have satisfactory energy to escape, thus it surrenders, which is formulated as:

$$x(t+1) = x_{prey}(t) - E|\Delta x(t)| \tag{13}$$

3.1.3. Soft Besiege with Progressive Rapid Dive

In this phase, the condition is valid when $r < 0$ and $|E_0| \geq 0$. Here, the prey's energy can permit it to escape successfully. Hawk tests the next move for performing the soft besiege phase that can be modeled as:

$$x(t+1) = x_{prey}(t) - E\left|Jx_{prey}(t) - x(t)\right| \tag{14}$$

$$Z = Y + S \times LF(D) \tag{15}$$

where LF indicates the levy flight function given in [34], D is the dimension and S represents a random vector by size $1 \times D$. In consequence, the following equation is obtained:

$$x(t+1) = \begin{cases} Yf(Y) < f(y(t)) \\ Zf(Z) < f(y(t)) \end{cases} \tag{16}$$

After simple substitution, the following formula is obtained:

$$x(t+1) = \begin{cases} x_{prey}(t) - E\left|Jx_{prey}(t) - x(t)\right| \ \forall f(Y) < f(y(t)) \\ Z = Y + S + LF(D) \ \ \forall f(Z) < f(y(t)) \end{cases} \tag{17}$$

3.1.4. Hard Besiege with Progressive Rapid Dive

When $r < 0$ and $|E_0| < 0$, the prey in this phase does not have the satisfactory energy to escape and a hard besiege is performed before the surprise pounce to chase and hunt the prey.

$$x(t+1) = \begin{cases} Yf(Y) < f(y(t)) \\ Zf(Z) < f(y(t)) \end{cases} \tag{18}$$

where Y and Z are obtained using new rules in Equations (19) and (20).

$$Y = x_{prey}(t) - E\left|Jx_{prey}(t) - x_m(t)\right| \tag{19}$$

$$Z = Y + S \times LF(D) \tag{20}$$

where $x_m(t)$ is calculated using Equation (9).

Figure 4 illustrates the pseudo-code of CHHO based PSS methodology.

3.2. Chaotic Maps

The Chaotic Map (CM) employment is one of the effective approaches to adjust some of the static parameters in metaheuristic algorithms and conquer early convergence. This domain has swiftly grown up to be a new research area in the recent optimization literature. In this work, CM is inserted into the original HHO to avoid trapping in a local optimum during the optimization process. Seven different CM types are attempted in this current study [35–39]: Iterative map, Gaussian map, Logistic map, Piecewise map, Singer map, Tent map, and Chebyshev map. The iterative map with infinite collapses can be written as described in Equation (21). However, the Gaussian map can be given in Equation (22). In addition, Logistic, Piecewise, Singer, Tent, and Chebyshev maps are defined as depicted in Equations (23)–(27), respectively.

Inputs: The maximum number of generations T and population size N

Outputs: The rabbit position and its final fitness value

Initialize the Hawks population via the proposed scheme.

while (Termination criterion is not met) **do**

  Determine the fitness values of hawks

  Set X_{rabbit} as the rabbit position (best position)

  for (each hawk (X_i)) **do**

    Update the jump strength J and initial energy E_0

    E_0 = 2rand()-1, J=2(1-rand())

    Update the E using Eq. (10)

    if (|E| ≥ 1) then ..... ▷ *Exploration phase*

      Update the position vector using Eq. (8)

    if (|E| < 1) then ..... ▷ *Exploitation phase*

      if (r ≥ 0.5 and |E| ≥ 0.5) then ..... ▷ *Soft besiege*

        Update the position vector using Eq. (12)

      else if (r ≥ 0.5 and |E| < 0.5) then ..... ▷ *Hard besiege*

        Update the position vector using Eq. (13)

      else if (r < 0.5 and |E| ≥ 0.5) then ..... ▷ *Soft besiege with progressive rapid dives*

        Update the location vector using Eq. (14)

      else if (r < 0.5 and |E| < 0.5) then ..... ▷ *Hard besiege with progressive rapid dives*

        Update the position vector using Eq. (18)

Return X_{rabbit} i.e., *Output*: best objective function value with optimal PSS parameters.

Figure 4. Pseudo-code of CHHO based PSS.

$$x_{t+1} = \sin\left(\frac{\gamma\pi}{x_t}\right) \tag{21}$$

$$x_{t+1} = \begin{cases} 0 \ \forall x_t = 0 \\ \frac{1}{x_t.mod(1)} \ Otherwise \end{cases} \tag{22}$$

$$x_{t+1} = a.x_t(1 - x_t) \tag{23}$$

$$x_{t+1} = \begin{cases} \frac{x_t}{P} \ 0 \le x_t < P \\ \frac{x_t - P}{0.5 - P} \ P \le x_t < 1/2 \\ \frac{1 - P - x_t}{0.5 - P} \ 1/2 \le x_t < 1 - P \\ \frac{1 - x_t}{P} \ 1 - P \le x_t < 1 \end{cases} \tag{24}$$

$$x_{i+1} = \mu\left(7.86x_i - 23.31x_i^2 + 28.75x_i^3 - 13.3x_i^4\right) \tag{25}$$

$$x_{i+1} = \begin{cases} \frac{x_i}{0.7 \ x_i < 0.7} \\ \frac{10}{3}(1 - x_i) \ x_i \ge 0.7 \end{cases} \tag{26}$$

$$x_{i+1} = \cos(k\cos^{-1}(x_k)) \tag{27}$$

Chaotic Harris Hawk's Optimizer

The traditional random initialization produces uncertain solution quality by guaranteeing the initial hawks distributed homogeneously in the search space. This consequence results because a part of the hawks is far away from the global optimum [39]. To overcome the above problem, the search space is selected such that it can be adjusted in the standard

HHO through chaotic maps techniques, this is the random of initial search space. In the enhanced algorithm, according to the ergodicity and non-repeatability of the chaos mechanism, it can accomplish overall searches at higher degrees than stochastic searches. The effort procedure is that hawk locations between the population are totally replaced by the mentioned chaotic maps, thus they masterly contribute to the search space. The misuse of CM produces a harmful influence on the main algorithm's working and may refute the above claims by disturbing the solution. So far, the main advantage of the CM is that the algorithm driven by CM encloses a smooth removal between exploitation and exploration. In the same way, the authors have used CM in this study to put back initial random parameters that perform the regular redistribution of the search space contrary to the original algorithm search with self-distributions. During the computation, HHO is combined with chaotic maps to cross the predicament of being trapped in local optima.

In the conventional HHO, the parameter of Equation (8) in the range of [0,1] is a random number. Here in the CHHO, it has been selected as chaotic numbers between 0 and 1, which is modeled as depicted in Equation (28).

$$x(t+1) = \begin{cases} CM(t) - r|x_{rand}(t) - 2r_2x(t)|q \geq 0.5 \\ x_{prey}(t) - x_a(t) - r_3(LB + r_4UB - LB))q < 0.5 \end{cases} \quad (28)$$

The question that now arises is: Can CHHO be used to produce purposive effects on the power system stability? This query rejoinder is sequentially consigned in the succeeding lines.

4. Results and Discussions

4.1. Solving the Benchmark Problems

This section examines in a few words the effectiveness of the proposed CM with HHO using benchmark functions. The unimodal benchmark functions are tabulated in Table 1, while multimodal and fixed-dimension (D) multimodal benchmark functions are described in detail in Ref. [38]. The results were achieved after 30 runs by each algorithm for all benchmark functions. It can be recognized from this Table that the results obtained with CHHO achieved a better value compared to the original HHO. The abbreviations of different algorithms under chaotic maps are arranged in Table 2.

Table 1. Description of unimodal benchmark functions.

ID	Formula	D	Range
F1	$f(x) = \sum_{i=1}^{n} x_i^2$	30	[100, 100]
F2	$f(x) = \sum_{i=1}^{n} \lvert x_i \rvert + \prod_{i=1}^{n} \lvert x_i \rvert$	30	[10, 10]
F3	$f(x) = \sum_{i=1}^{n} \left(\sum_{j-1}^{i} x_j \right)^2$	30	[100, 100]
F4	$f(x) = max_i\{\lvert x_i \rvert, 1 \leq i \leq n\}$	30	[100, 100]
F5	$f(x) = \sum_{i=1}^{n-1} \left[100\left(x_{i+1} - x_i^2\right)^2 + (x_i - 1)^2 \right]$	30	[30, 30]
F6	$f(x) = \sum_{i=1}^{n} (\lvert x_i + 0.5 \rvert)^2$	30	[100, 100]
F7	$f(x) = \sum_{i=1}^{n} ix_i^4 + random(0, 1)$	30	[1.28, 1.28]

Table 2. The abbreviations of different algorithms.

Chaotic Map Abbreviation	Gauss/Mouse CHHO-1	Iterative CHHO-2	Logistic CHHO-3	Piecewise CHHO-4
Chaotic Map Abbreviation	Tent CHHO-5	Chebyshev Map CHHO-6	Singer CHHO-7	

Based on the numerical results obtained in Table 3, it can be said that these results corroborate the applicability of the suggested approaches that have the ability to reach the global optimum for the mentioned functions. Surprisingly, amid the CM applied here, the Piecewise map impressively produced better solution quality in solving unconstrained global optimization problems and can reinforce search strength in problem space. Accordingly, it has the capacity to reach the exact solution through a swift balance among the global and local search. This prosperity demonstrates the superiority of this map at improving the intensification and diversification capacities and for this reason; our choice is supervened by the Piecewise map, which will be applied to the power system stability problem in the next sections. As, we can also perceive, other chaotic maps can definitely increase the competence of HHO with the exception of the Singer map, which seems not able to attain the global minimum in the same functions.

4.2. Solving the Power System Stability Problem

In this subsection, HHO is improved by means of chaotic maps to improve the search strategy during the optimization procedure for ensuring optimal parameters of PSS design by taking into account the performance of the plant. A parallel simulation was carried out with HHO and DE algorithms [40] to contrast the proposed CHHO's effectiveness. The specification of each algorithm is proffered as follows: The population and the maximum number of iterations for each algorithm are 100 and 100, respectively.

The declared design scheme applied to the 10 generators will attest to its capacity to be adequately effective against challenges in executing this method on larger power systems. The efficacy of the proposed PSS tuning is validated by applying a three-phase fault with a duration of 90 ms in the middle of the transmission line that linked bus 28 and bus 29 without line tripping under the two operating conditions that are given in Table 4.

The evolution of the objective function depending on the number of generations is given in Figure 5 using different algorithms. As we shown in this figure, the minimum fitness value is procured using CHHO with the best convergence compared to standard HHO and DE, these results are due to the perfection of the HHO global search by CM, which is worthily accomplished in the optimal solution. Also, CM in HHO presides over the speedy convergence to its global optimality and outfits a switch ploy for the HHO mechanism in the exploration phase that prevents getting stuck in a fake solution. At this juncture, HHO falls in the partial solution region, which emphasizes the importance of CM in handling the HHO deficiency. The optimal parameters discovered by the proposed algorithms are shown in Table 5.

The system response of speed deviation with different algorithms under the disturbance of operating condition 1 is shown in Figure 6. Proceeding from the simulation outcomes, the speed deviation using HHO-PSS adequately achieves acceptable damping but with a slow response. Otherwise, it can be observed that the system employed with CHHO-PSS broadly afforded excellent system oscillation suppression in the power system with the best control signal, plus it has a faster response and more damping proficiency when compared with other algorithms. This score categorically matches a much higher damping factors ratio value. Whereas, the system oscillation is not mitigated in case of the model without a stabilizer due to the severe outage considered and may degrade the power system operations. Thus, this consequence affirms the superiority of the proposed integration of chaotic maps with HHO in attaining the optimal PSS parameters judged against the standard algorithm.

Table 3. Results of the comparative methods on the seven Unimodal benchmark functions.

Fun No.	Measure	Comparative Methods				
		HHO	**CHHO-1**	**CHHO-2**	**CHHO-3**	**CHHO-4**
F1	Worst	5.9512E-98	6.2863E-99	2.0103E-101	1.4375E-96	1.2982E-98
	Average	2.1231E-99	2.3526E-100	6.7031E-103	5.0425E-98	4.9799E-100
	Best	7.1842E-116	1.6451E-117	2.1923E-116	3.5854E-115	6.9534E-117
	STD	1.0866E-98	1.1470E-99	3.6703E-102	2.6218E-97	2.3706E-99
F2	Worst	1.1163E-51	1.0805E-50	3.2310E-51	2.9698E-52	1.1735E-50
	Average	4.5206E-53	3.6432E-52	1.2862E-52	1.4932E-53	9.3781E-52
	Best	5.7801E-61	1.1577E-61	1.2640E-61	8.5916E-60	2.1624E-61
	STD	2.0413E-52	1.9719E-51	5.9441E-52	5.6740E-53	2.9137E-51
F3	Worst	1.0396E-79	8.1627E-80	7.3443E-82	1.5567E-77	1.8161E-81
	Average	3.6221E-81	2.7210E-81	2.4492E-83	5.1889E-79	6.0619E-83
	Best	1.7647E-101	2.0509E-106	1.7460E-102	6.6822E-103	2.7971E-105
	STD	1.8970E-80	1.4903E-80	1.3409E-82	2.842048E-78	3.3156E-82
F4	Worst	2.4929E-49	4.3522E-51	3.4972E-49	2.4458E-51	3.3407E-50
	Average	9.4099E-51	3.2296E-52	1.7949E-50	1.8715E-52	1.5649E-51
	Best	2.5972E-61	1.8244E-58	6.3810E-60	8.2259E-59	2.1513E-59
	STD	4.5453E-50	8.6567E-52	7.0223E-50	5.1596E-52	6.2276E-51
F5	Worst	1.8347e-02	2.0060e-02	2.8406e-02	1.4052e-02	5.2828e-02
	Average	5.4907e-03	4.9067e-03	5.4719e-03	3.3413e-03	4.8627e-03
	Best	1.1860E-05	7.7402E-06	2.1216E-05	5.3116E-06	2.5568E-06
	STD	4.8108e-03	6.6480e-03	6.6148e-03	4.0093e-03	1.0959e-02
F6	Worst	1.2227E-04	2.3521E-04	2.4992E-04	3.9409E-04	2.3173E-04
	Average	4.0938E-05	5.0787E-05	5.0576E-05	5.8620E-05	4.4138E-05
	Best	6.9660E-07	3.1519E-07	2.3501E-07	4.2052E-07	1.2151E-08
	STD	3.7858E-05	6.1788E-05	6.4697E-05	9.3447E-05	6.1991E-05
F7	Worst	5.8867E-04	5.4054E-04	3.7393E-04	3.7813E-04	1.8347E-04
	Average	9.8557E-05	8.9911E-05	9.4252E-05	7.0464E-05	7.0338E-05
	Best	4.4691E-06	3.6960E-07	4.2456E-06	2.5632E-06	1.6094E-06
	STD	1.1274E-04	1.1106E-04	8.3870E-05	7.3039E-05	5.4223E-05

Fun No.	Measure	Comparative Methods			
		CHHO-5	**CHHO-6**	**CHHO-7**	**DE**
F1	Worst	6.7354E-99	2.6433E-100	8.2943E-91	4.4386E-25
	Average	2.2975E-100	1.3653E-101	2.7648E-92	6.0132E-26
	Best	1.0114E-118	8.8329E-120	1.6735E-116	7.6612E-29
	STD	1.2289E-99	5.2446E-101	1.5143E-91	1.0144E-25
F2	Worst	3.9850E-51	4.0036E-52	1.1014E-50	3.3423E-15
	Average	1.6746E-52	3.0616E-53	5.7821E-52	9.5648E-16
	Best	1.0731E-59	1.9621E-61	6.4599E-62	1.5947E-16
	STD	7.4429E-52	8.3276E-53	2.2698E-51	7.0237E-16
F3	Worst	1.6772E-82	6.4230E-83	3.6351E-82	2.4213E+00
	Average	5.8498E-84	2.1699E-84	1.2361E-83	7.0300E-01
	Best	5.2052E-105	1.3792E-105	1.0633E-106	6.9908E-02
	STD	3.0604E-83	1.1722E-83	6.6335E-83	6.1012E-01
F4	Worst	3.7611E-48	3.8207E-51	8.8826E-50	3.4902E+01
	Average	1.2607E-49	1.7452E-52	3.1797E-51	2.2957E+01
	Best	1.7699E-59	1.1496E-59	2.6430E-59	1.2265E+01
	STD	6.8655E-49	7.0775E-52	1.6195E-50	6.0491E+00
F5	Worst	4.1583e-02	2.9487e-02	1.5495e-02	2.8483e+01
	Average	4.6260e-03	4.6260e-03	3.8083e-03	9.0975e+00
	Best	2.0791E-05	5.5753E-06	1.2397E-09	3.7867E-07
	STD	8.0860e-03	6.5421e-03	3.9882e-03	1.0201e+01
F6	Worst	2.3884E-04	1.8382E-04	2.0349E-04	3.4512E-2
	Average	3.9667E-05	4.5621E-05	4.4487E-05	7.3124E-2
	Best	3.3941E-07	1.9629E-07	8.9470E-08	1.1468E-3
	STD	5.5406E-05	5.3004E-05	5.2918E-05	8.2926E-2
F7	Worst	4.5400E-04	3.4588E-04	5.0626E-04	9.7697E-03
	Average	9.7567E-05	8.4010E-05	7.6508E-05	4.1090E-03
	Best	2.8635E-06	6.0441E-06	2.5048E-06	1.2936E-03
	STD	1.0110E-04	8.9123E-05	9.2046E-05	1.8296E-03

Table 4. System loading conditions to test the power system.

Operating Condition 1	Operating Condition 2
Nominal active power Nominal reactive power	Total active power increasing by 12% Total reactive power increasing by 10%

Table 5. Optimal parameters for operating condition 1.

Methods	Parameter	Generators (1 → 5)				
		G1	G2	G3	G4	G5
CHHO	K_m	43.4310	14.2737	37.7955	31.4291	7.9842
	T_{1m}	0.4060	0.9068	0.7550	0.9514	0.6082
	T_{2m}	0.3832	0.8726	0.7552	0.3045	0.6443
	T_{3m}	0.9012	0.9216	0.8028	0.2667	0.4596
	T_{4m}	0.8028	0.5811	0.7651	0.6839	0.2440
HHO	K_m	57.5282	37.1416	61.9856	63.4233	29.6652
	T_{1m}	1.5043	0.7014	0.7549	0.4732	1.0661
	T_{2m}	1.6216	0.7173	1.1082	0.8383	1.5622
	T_{3m}	0.5159	0.4590	0.8203	0.7823	0.8478
	T_{4m}	0.5871	0.6144	1.5961	1.3040	1.4983
DE	K_m	60.5909	74.2482	39.1043	36.8485	96.4407
	T_{1m}	1.5587	1.7429	1.0596	1.4793	1.7632
	T_{2m}	0.0100	0.2594	0.0769	0.7508	0.0100
	T_{3m}	1.3167	1.8000	1.8000	1.5217	1.4877
	T_{4m}	0.1503	0.0100	0.0100	0.0100	0.3046
Methods	**Parameter**	**Generators (6 → 10)**				
		G6	**G7**	**G8**	**G9**	**G10**
CHHO	K_m	19.1182	10.3593	25.3833	28.9654	21.2603
	T_{1m}	0.1737	0.8911	0.9673	0.8191	0.5594
	T_{2m}	0.6261	0.5999	0.8608	0.8438	0.4783
	T_{3m}	0.9334	0.8269	0.3875	0.7079	0.4624
	T_{4m}	0.4554	0.3653	0.7269	0.6510	0.3156
HHO	K_m	69.6979	77.4696	14.8654	47.4786	65.7820
	T_{1m}	0.4262	0.3678	0.8822	0.6309	0.8029
	T_{2m}	1.6650	1.5090	1.3877	1.2049	1.1785
	T_{3m}	0.9562	0.7730	1.0435	0.5317	1.1891
	T_{4m}	0.7546	0.4548	1.3494	0.3721	0.7900
DE	K_m	24.1492	100.0000	16.5280	76.4606	97.8444
	T_{1m}	1.8000	0.3468	1.4932	1.5531	1.0735
	T_{2m}	0.0100	0.0100	0.0100	0.0100	0.1508
	T_{3m}	1.8000	1.1243	0.7494	0.2000	0.5241
	T_{4m}	0.6028	0.9743	0.0822	0.0100	0.3192

The system response of speed deviation with different algorithms under the disturbance of operating condition 1 is shown in Figure 6. Proceeding from the simulation outcomes, the speed deviation using HHO-PSS adequately achieves acceptable damping but with a slow response. Otherwise, it can be observed that the system employed with CHHO-PSS broadly afforded excellent system oscillation suppression in the power system with the best control signal, plus it has a faster response and more damping proficiency when compared with other algorithms. This score categorically matches a much higher damping factors ratio value. Whereas, the system oscillation is not mitigated in case of the model without stabilizer due to the severe outage considered and may degrade the power system operations. Thus, this consequence affirms the superiority of the proposed integration of chaotic maps with HHO in attaining the optimal PSS parameters judged against the standard algorithm.

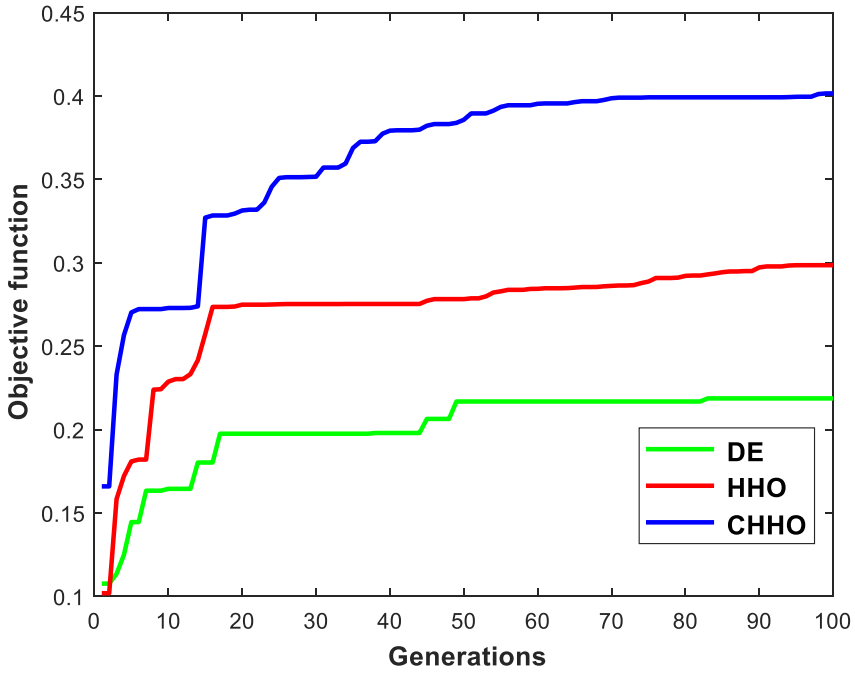

Figure 5. Convergence curves of objective function.

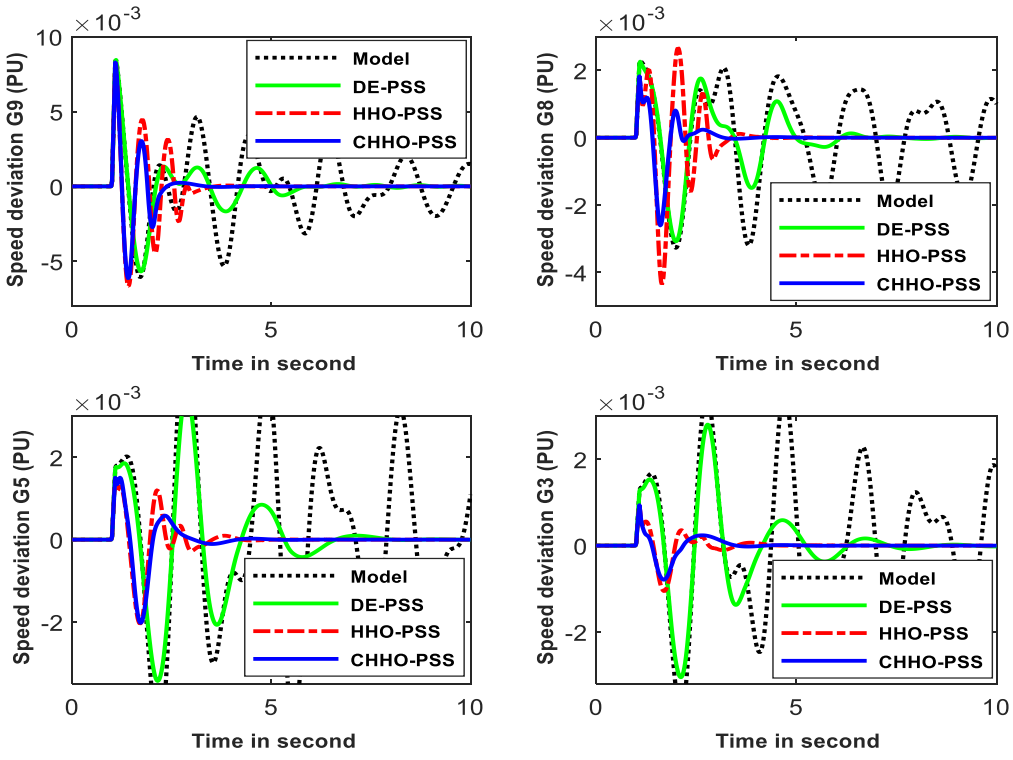

Figure 6. Speed deviation responses of the system under operating condition 1.

Figure 7 illustrates the system response of speed deviation with different algorithms under the disturbance of operating condition 2. The simulation results obtained clearly indicate that the system response is greatly improved with the proposed CHHO-PSS in terms of settling time and overshoots, and it speedily reached the steady state in comparison with another algorithm. Hence, we can partially accept that the system equipped with CHHO-PSS supplies superior damping characteristics of electromechanical modes and it attains transient stability rapidly compared to HHO-PSS and DE-PSS, which proves that the iterative map gives a suitable improvement. The appreciation assortment of PSS

parameters leads to satisfactory robustness. With regards again to these figures, it can also be noticed that the test system without any stabilizer is unstable and the generator has lost its synchronism.

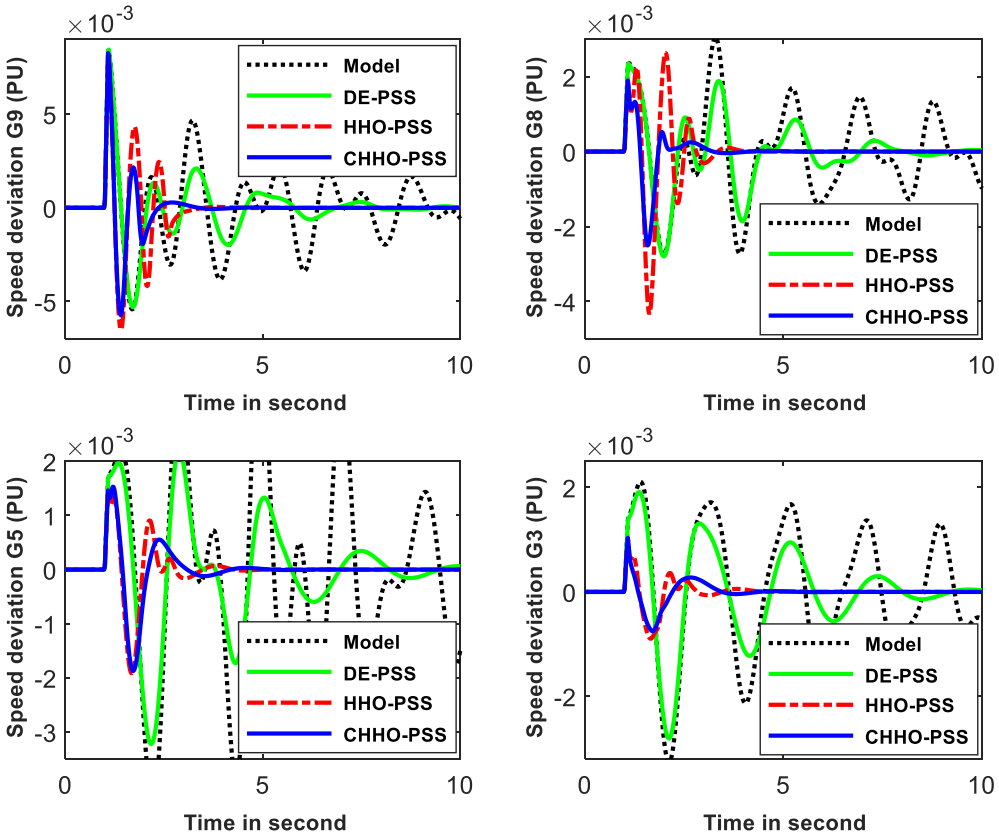

Figure 7. Speed deviation responses of the system under operating condition 2.

The model eigenvalues with the suggested PSS tuning for mentioned systems are revealed in Figures 8 and 9 showing the eigenvalues of the electromechanical mode through damping ratios axes for the two studied conditions, respectively. From a general point of view, the results above indicate that the power system without PSS is installed. It can be seen that the modes are badly damped for two operating conditions with the intention that the power system is clearly unstable. On the other hand, it can be understood that all electromechanical modes with mentioned CHHO-PSS including local and interregional modes are appreciably moved to the left side in the s-plane by enhancing concurrently both damping ratio and the eigenvalues real-part in which the least damping ratio is skipped up 40 % for two operating conditions. The perfection resulting from the linear model is in superior approval compared with that obtained by the nonlinear model. The full view of the results demonstrates the inherent strengths of the suggested chaotic map to obtain the best power system stability and refine the HHO drawback.

For more testing the system response preciseness in time-domain simulation, the performance index includes the Integral Squared Error (ISE). Integral Absolute Error (IAE). Integral of Time multiplied by the Squared Error ($ITSE$) and Integral of the Time-Weighted Absolute Error ($ITAE$) are performed for statistically analyzing the effectiveness of the proposed stabilizers and is given as:

$$ISE = \int_0^{tsim} e(t)^2 dt \tag{29}$$

$$IAE = \int_0^{tsim} |e(t)| dt \tag{30}$$

$$ITAE = \int_0^{tsim} t|e(t)|dt \tag{31}$$

$$ITSE = \int_0^{tsim} te(t)^2 dt \tag{32}$$

where t_{sim} is total simulation time and $|e|$ symbolizes the absolute error.

Whereas, the performance indices and settling time (T_S) values calculated for the speed response of mentioned generators under system study with CHHO-PSS and HHO-PSS are specified in Table 6.

The robustness and notability of the proposed controller are evaluated through Figure of Demerit (FD) analysis based on the system performance index and being used by:

$$FD = ((200 \times OS_i)^2 + \left(200 \times US_i\right)^2 + 0.5 \times T_{Si}^2\Big) \tag{33}$$

where Undershoot (US) and Overshoot (OS) are the characteristics of speed deviation responses.

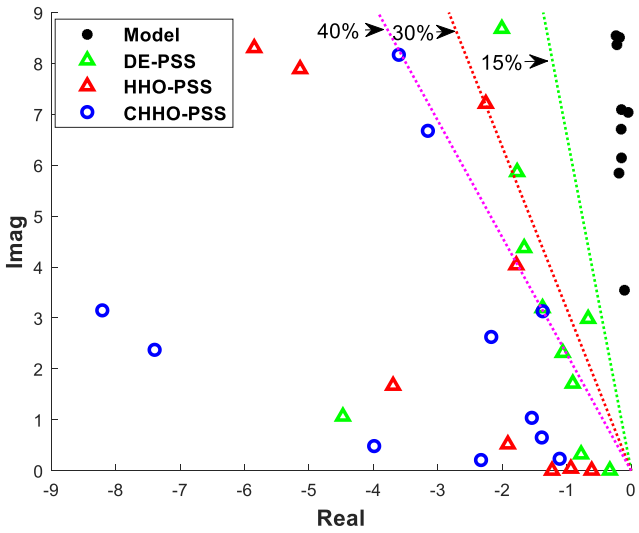

Figure 8. Eigenvalues distribution of electromechanical modes under operating condition 1.

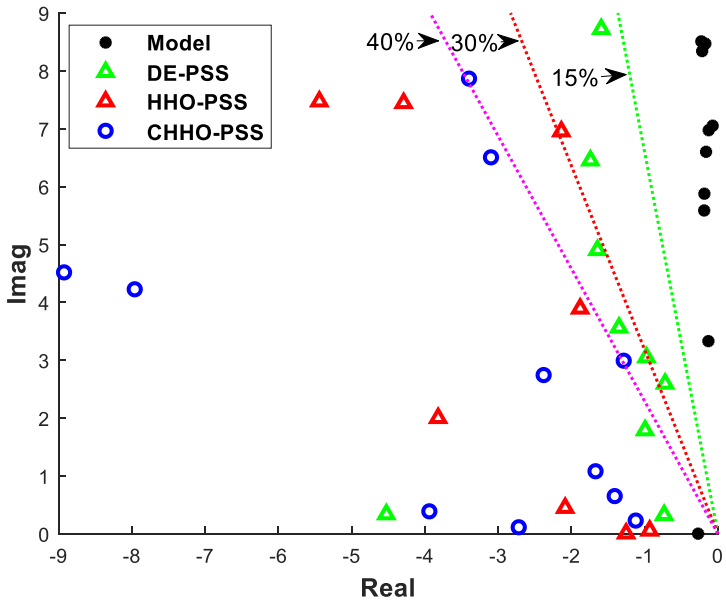

Figure 9. Eigenvalues distribution of electromechanical modes under operating condition 2.

Table 6. T_S and Performance index values under different algorithms.

Generator	Algorithms	Ts (s)	Peak	IAE	ISE	ISE	ITAE	FD
G9	CHHO	**2.9775**	**0.0083**	**0.1925**	**8.05E-4**	**2.0157**	**0.2968**	**2.0160**
	HHO	3.2979	0.0083	0.2876	0.0012	2.989	0.5111	2.2307
	DE	5.6727	0.0085	0.3646	0.0013	3.1324	0.925	4.6352
G8	CHHO	**3.0501**	**0.0026**	**0.07**	**9.68E-5**	**0.2426**	**0.1176**	**2.2142**
	HHO	3.7309	0.0044	0.1531	3.25E-4	0.8145	0.2939	2.2963
	DE	6.6078	0.0031	0.2337	3.63E-4	0.9082	0.6571	**4.7115**
G5	CHHO	**3.9285**	**0.0020**	**0.0765**	**8.83E-5**	**0.2211**	**0.1393**	**1.9250**
	HHO	4.0927	0.0020	0.0812	9.24E-5	0.2314	0.152	2.9314
	DE	7.5183	0.0035	0.3309	6.65E-4	1.6651	0.9871	3.8999
G3	CHHO	**3.9123**	**9.37E-4**	**0.0347**	**1.56E-5**	**3.91E-2**	**6.80E-2**	**5.7327**
	HHO	4.2944	0.0011	0.0403	2.24E-5	5.61E-02	7.82E-2	6.2001
	DE	7.8745	0.0031	0.2551	4.16E-4	1.0416	0.7517	7.0259

Taking a closer look at these values. It can be deduced that the proposed stabilizer using the CHHO achieves a minimum value of performance indices. it can also be observed that the minimum value of T_S is obtained by the same algorithm-based PSS. These numerical results obviously substantiate that CHHO outperforms HHO and DE in terms of settling time and error. The aforementioned confirm that the CM helps in decreasing the probability and assumption of HHO trapped in local minima through mutation of internal control mechanism. Numerical results of FD-based system performance under different operating conditions and cases are revealed in the last column of Table 6. From the test case results. the designed control strategy achieved the best FD value for all cases that can be clearly matched to the most excellent response obtained in which has a concurrently small settling time, overshoot, and undershoot compared to other algorithms. In addition, the proposed methodology plays an important role in the robust stable operation of power the system in diverse operating conditions. Hence, the outstanding and efficacious signal supplied from CHHO-PSS assists significantly in limiting the electromechanical oscillations.

5. Concluding Remarks and Future Work

Seven chaotic maps have been successfully implemented to enhance the standard HHO and to achieve the optimal PSS tuning in a multimachine power system. First, an unconstrained mathematical problem has been chosen to prove the applicability of this proposition. Then, the application of the proposed CHHO is tested on a five-machine and eight-bus power system under different loading conditions. The CHHO is applied to find the optimal PSS parameters, which were set to the damping ratio of lightly damped electromechanical modes in order to provide satisfactory damping oscillations. The performance of the proposed CHHO-PSS has been compared with HHO-PSS and DE through eigenvalue analysis and nonlinear simulation. In addition. the performance of CHHO-PSS is analyzed by using the performance indices and settling time as the least value and compared to HHO-PSS and DE-PSS. The calculation of Figure of Demerit is conducted to indicate the advantages of the proposed CHHO-PSS based methodology. The best simulation results clearly manifest in the robustness of the mentioned methodology for improving to a great extent the dynamic stability of the power system under different cases studies. It is planned to extend this current work to attempt many more chaotic maps with further analysis. In addition to that, it has been planned to apply the optimization technique to solve larger systems such as a 14-machine and 39-bus network. Further verification either by using experimental tests or real-time hardware in the loop simulations can be extended as future work.

Author Contributions: Conceptualization, L.C., A.C., S.A. and A.E.-F.; methodology, H.G.Z., S.S.M.G., L.C., A.C. and S.A.; software, L.C., A.C. and S.A.; validation, A.E.-F., H.G.Z. and S.S.M.G.; formal analysis. L.C., A.C., S.A. and A.E.-F.; investigation, H.G.Z. and S.S.M.G.; resources, H.G.Z. and S.S.M.G.; data curation, L.C., A.C., S.A. and A.E.-F.; writing—original draft preparation, L.C., A.C., S.A. and A.E.-F.; writing—review and editing, H.G.Z. and S.S.M.G.; visualization, L.C., A.C. and S.A.; supervision, A.E.-F. and S.S.M.G.; project administration, A.E-F. and S.S.M.G.; funding acquisition, H.G.Z. and S.S.M.G. All authors have read and agreed to the published version of the manuscript.

Funding: This project is funded by the Taif University Researchers Supporting Project under Grant TURSP-2020/345. Taif. Saudi Arabia.

Institutional Review Board Statement: The study did not involve humans or animals.

Informed Consent Statement: The study did not involve humans.

Data Availability Statement: Not applicable.

Acknowledgments: The authors would like to acknowledge the financial support received from Taif University Researchers Supporting Project Number (TURSP-2020/345). Taif University. Taif. Saudi Arabia.

Conflicts of Interest: The authors declare no conflict of interest.

References

1. Shafiullah, M.; Rana, M.J.; Alam, M.S.; Abido, M.A. Online tuning of power system stabilizer employing genetic programming for stability enhancement. *J. Electr. Syst. Inf. Technol.* **2018**, *5*, 287–299. [CrossRef]
2. Hassan, L.H.; Moghavvemi, M.; Almurib, H.; Muttaqi, K.; Ganapathy, V.G. Optimization of power system stabilizers using participation factor and genetic algorithm. *Int. J. Electr. Power Energy Syst.* **2014**, *55*, 668–679. [CrossRef]
3. Benasla, M.; Denaï, M.; Liang, J.; Allaoui, T.; Brahami, M. Performance of wide-area power system stabilizers during major system upsets: Investigation and proposal of solutions. *Electr. Eng.* **2021**, *103*, 1417–1431. [CrossRef]
4. Zhang, Y.; Malik, O.P.; Hope, G.S.; Chen, G.P. Application of an inverse input/output mapped ANN as a power system stabilizer. *IEEE Trans. Energy Convers.* **1994**, *9*, 433–441. [CrossRef]
5. He, J.; Malik, O.P. An adaptive power system stabilizer based on recurrent neural networks. *IEEE Trans. Energy Convers.* **1997**, *12*, 413–418. [CrossRef]
6. Gupta, A.; Gurrala, G.; Sastry, P.S. An Online Power System Stability Monitoring System Using Convolutional Neural Networks. *IEEE Trans. Power Syst.* **2018**, *34*, 864–872. [CrossRef]
7. Al-Duwaish, H.N.; Al-Hamouz, Z.M. A neural network based adaptive sliding mode controller: Application to a power system stabilizer. *Energy Convers. Manag.* **2011**, *52*, 1533–1538. [CrossRef]
8. El-Zonkoly, A.; Khalil, A.; Ahmied, N. Optimal tunning of lead-lag and fuzzy logic power system stabilizers using particle swarm optimization. *Expert Syst. Appl.* **2009**, *36*, 2097–2106. [CrossRef]
9. Ghasemi, A.; Shayeghi, H.; Alkhatib, H. Robust design of multimachine power system stabilizers using fuzzy gravitational search algorithm. *Int. J. Electr. Power Energy Syst.* **2013**, *51*, 190–200. [CrossRef]
10. Saoudi, K.; Harmas, M. Enhanced design of an indirect adaptive fuzzy sliding mode power system stabilizer for multi-machine power systems. *Int. J. Electr. Power Energy Syst.* **2014**, *54*, 425–431. [CrossRef]
11. Nechadi, E.; Harmas, M.; Hamzaoui, A.; Essounbouli, N. A new robust adaptive fuzzy sliding mode power system stabilizer. *Int. J. Electr. Power Energy Syst.* **2012**, *42*, 1–7. [CrossRef]
12. Chaturvedi, D.K.; Malik, O.P. Neurofuzzy Power System Stabilizer. *IEEE Trans. Energy Convers.* **2008**, *23*, 887–894. [CrossRef]
13. Bhati, P.; Gupta, R. Robust fuzzy logic power system stabilizer based on evolution and learning. *Int. J. Electr. Power Energy Syst.* **2013**, *53*, 357–366. [CrossRef]
14. Jebali, M.; Kahouli, O.; Abdallah, H.H. Optimizing PSS parameters for a multi-machine power system using genetic algorithm and neural network techniques. *Int. J. Adv. Manuf. Technol.* **2016**, *90*, 2669–2688. [CrossRef]
15. Farah, A.; Guesmi, T.; Abdallah, H.H.; Ouali, A. A novel chaotic teaching–learning-based optimization algorithm for multi-machine power system stabilizers design problem. *Int. J. Electr. Power Energy Syst.* **2016**, *77*, 197–209. [CrossRef]
16. Mohammadi, M.; Ghadimi, N. Optimal location and optimized parameters for robust power system stabilizer using honeybee mating optimization. *Int. Trans. Elect. Energy Syst.* **2015**, *21*, 242–258. [CrossRef]
17. Chitara, D.; Swarnkar, A.; Gupta, N.; Niazi, K.; Bansal, R. Optimal Tuning of Multimachine Power System Stabilizer using Cuckoo Search Algorithm. *IFAC-PapersOnLine* **2015**, *48*, 143–148. [CrossRef]
18. Wang, D.; Ma, N.; Wei, M.; Liu, Y. Parameters tuning of power system stabilizer PSS4B using hybrid particle swarm optimization algorithm. *Int. Trans. Elect. Energy Syst.* **2018**, *28*, e2598. [CrossRef]
19. Dasu, B.; Sivakumar, M.; Rao, R.S. Design of robust modified power system stabilizer for dynamic stability improvement using Particle Swarm Optimization technique. *Ain Shams Eng. J.* **2019**, *10*, 769–783. [CrossRef]

20. Shayeghi, H.; Ghasemi, A. A multi objective vector evaluated improved honey bee mating optimization for optimal and robust design of power system stabilizers. *Int. J. Electr. Power Energy Syst.* **2014**, *62*, 630–645. [CrossRef]
21. Jordehi, A.R. Optimal setting of TCSCs in power systems using teaching–learning-based optimisation algorithm. *Neural Comput. Appl.* **2014**, *26*, 1249–1256. [CrossRef]
22. Sabo, A.; Wahab, N.I.A.; Othman, M.L.; Jaffar, M.Z.A.M.; Beiranvand, H. Optimal design of power system stabilizer for multimachine power system using farmland fertility algorithm. *Int. Trans. Electr. Energy Syst.* **2020**, *30*, e12657. [CrossRef]
23. Dasu, B.; Sivakumar, M.; Srinivasarao, R. Interconnected multi-machine power system stabilizer design using whale optimization algorithm. *Prot. Control. Mod. Power Syst.* **2019**, *4*, 2. [CrossRef]
24. Sambariya, D.; Prasad, R. Robust tuning of power system stabilizer for small signal stability enhancement using metaheuristic bat algorithm. *Int. J. Electr. Power Energy Syst.* **2014**, *61*, 229–238. [CrossRef]
25. Ali, E. Optimization of Power System Stabilizers using BAT search algorithm. *Int. J. Electr. Power Energy Syst.* **2014**, *61*, 683–690. [CrossRef]
26. Chaib, L.; Choucha, A.; Arif, S. Optimal design and tuning of novel fractional order PID power system stabilizer using a new metaheuristic Bat algorithm. *Ain Shams Eng. J.* **2017**, *8*, 113–125. [CrossRef]
27. Tolstolesova, L.A.; Yumanova, N.N.; Mazikova, E.V.; Glukhikh, I.N.; Vorobieva, M.S. Realization of PPP projects in the sector of energetics as a condition of a sustainable development of macroregions. *Entrep. Sustain. Issues* **2019**, *7*, 263–277. [CrossRef]
28. Plėta, T.; Tvaronavičienė, M.; Della Casa, S.; Agafonov, K. Cyber-attacks to critical energy infrastructure and management issues: Overview of selected cases. *Insights Into Reg. Dev.* **2020**, *2*, 703–715. [CrossRef]
29. Mondal, D.; Chakrabarti, A.; Sengupta, A. *Power System Small Signal Stability Analysis and Control*, 2nd ed.; Academic Press: Cambridge, MA, USA, 9 March 2020; ISBN -10.
30. Rahmatian, M.; Seyedtabaii, S. Multi-machine optimal power system stabilizers design based on system stability and nonlinearity indices using Hyper-Spherical Search method. *Int. J. Electr. Power Energy Syst.* **2018**, *105*, 729–740. [CrossRef]
31. Islam, N.N.; Hannan, M.A.; Shareef, H.; Mohamed, A. An application of backtracking search algorithm in designing power system stabilizers for large multi-machine system. *Neurocomputing* **2017**, *237*, 175–184. [CrossRef]
32. Butti, D.; Mangipudi, S.K.; Rayapudi, S.R. An improved whale optimization algorithm for the design of multi-machine power system stabilizer. *Int. Trans. Electr. Energy Syst.* **2020**, *30*, e12314. [CrossRef]
33. Heidari, A.A.; Mirjalili, S.; Faris, H.; Aljarah, I.; Mafarja, M.; Chen, H. Harris hawks optimization: Algorithm and applications. *Futur. Gener. Comput. Syst.* **2019**, *97*, 849–872. [CrossRef]
34. Abdel-Basset, M.; Mohamed, R.; Abouhawwash, M.; Nam, Y.; El-Fergany, A. Recent Meta-Heuristic Algorithms with a Novel Premature Covergence Method for Determining the Parameters of PV Cells and Modules. *Electronics* **2021**, *10*, 1846. [CrossRef]
35. Bentouati, B.; Javaid, M.S.; Bouchekara, H.R.E.H.; El-Fergany, A.A. Optimizing performance attributes of electric power systems using chaotic salp swarm optimizer. *Int. J. Manag. Sci. Eng. Manag.* **2019**, *15*, 165–175. [CrossRef]
36. Ewees, A.A.; el Aziz, M.A.; Hassanien, A.E. Chaotic multi-verse optimizer-based feature selection. *Neural Comput. Appl.* **2017**, *31*, 991–1006. [CrossRef]
37. Sayed, G.I.; Tharwat, A.; Hassanien, A.E. Chaotic dragonfly algorithm: An improved metaheuristic algorithm for feature selection. *Appl. Intell.* **2018**, *49*, 188–205. [CrossRef]
38. Abualigah, L.; Yousri, D.; Elaziz, M.A.; Ewees, A.A.; Al-Qaness, M.A.; Gandomi, A.H. Aquila Optimizer: A novel meta-heuristic optimization algorithm. *Comput. Ind. Eng.* **2021**, *157*, e107250. [CrossRef]
39. Abdel-Basset, M.; Mohamed, R.; El-Fergany, A.; Chakrabortty, R.K.; Ryan, M.J. Adaptive and Efficient optimization model for optimal parameters of proton exchange membrane fuel cells: A comprehensive analysis. *Energy* **2021**, *233*, e121096. [CrossRef]
40. Ghoneim, S.; Kotb, M.; Hasanien, H.; Alharthi, M.; El-Fergany, A. Cost Minimizations and Performance Enhancements of Power Systems Using Spherical Prune Differential Evolution Algorithm Including Modal Analysis. *Sustainability* **2021**, *13*, 8113. [CrossRef]